THE JOURNAL OF PHYSICAL CHEMISTRY C

Article

pubs.acs.org/JPCC

Stochastic Pore Blocking and Gating in PDMS–Glass Nanopores from Vapor–Liquid Phase Transitions

Steven Shimizu,[†] Mark Ellison,[‡] Kimberly Aziz,[†] Qing Hua Wang,[†] Zachary Ulissi,[†] Zachary Gunther,[†] Darin Bellisario,[†,§] and Michael Strano*,[†]

[†]Department of Chemical Engineering, Massachusetts Institute of Technology, Cambridge, Massachusetts 02139, United States

[‡]Department of Chemistry, Ursinus College, Collegeville, Pennsylvania 19426, United States

[§]Department of Chemistry, Massachusetts Institute of Technology, Cambridge, Massachusetts 02139, United States

Supporting Information

ABSTRACT: Polydimethylsiloxane (PDMS) is commonly used in research for microfluidic devices and for making elastomeric stamps for soft lithography. Its biocompatibility and nontoxicitiy also allow it to be used in personal care, food, and medical products. Herein we report a phenomenon observed when patch clamp, a technique normally used to study biological ion channels, is performed on both grooved and planar PDMS surfaces, resulting in stochastic current fluctuations that are due to a nanopore being formed at the interface of the PDMS and glass surfaces and being randomly blocked. Deformable pores between 1.9 ± 0.7 and 7.4 ± 2.1 nm in diameter, depending on the calculation method, form upon patching to the surface. Coulter blocking and nanoprecipitation are ruled out, and we instead propose a mechanism of stochastic current fluctuations arising from transitions between vapor and liquid phases, consistent with similar observations and theory from statistical mechanics literature. Interestingly, we find that $[Ru(bpy)_3]^{2+}$, a common probe molecule employed in nanopore research, physisorbs inside these hydrophobic nanopores blocking all ionic current flow at concentrations higher than 1×10^{-4} M, despite the considerably larger pore diameter relative to the molecule. Patch clamp methods are promising for the study of stochastic current fluctuations and other transport phenomenon in synthetic nanopore systems.

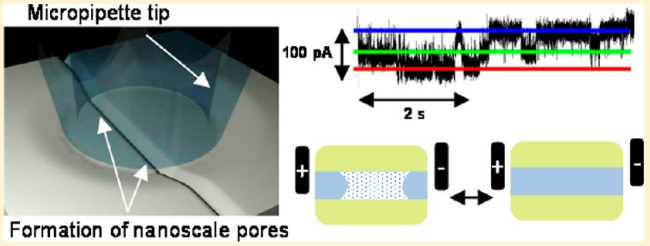

INTRODUCTION

There is significant interest in the use of isolated, synthetic nanopores for separation and analytical applications.[1−4] It is of particular interest to study the voltage-driven transport properties of these nanopores through a voltage-clamp apparatus, as this allows high-fidelity electronic readout corresponding to the current moving through the pore. These measurements have demonstrated several interesting transport properties and regimes found inside nanopores, including stochastic ion pore-blocking,[5−7] nanoprecipitation, and electric field-induced wetting/dewetting.[8] Nearly all of these isolated, synthetic nanopores consist of the following materials systems: carbon nanotubes,[7] SiN or SiO_2 nanopores,[9] and track-etched polymer membranes.[10]

Patch clamp is a widely used technique in electrophysiology to monitor ionic currents and the kinetics of channel opening through biological ion channels in cell membranes. In this technique, a micropipet is patched onto a very small section of the cell membrane under voltage clamp conditions.[11] However, its application to synthetic nanopores has been investigated only in a few cases.[12,13] The stochastic nature of biological ion channel gating has been studied extensively in the literature and is usually attributed to a conformational change in the protein ion channel; various ion channels can be activated by transmembrane potentials, ligands binding to receptors on ion channels, and other stimuli. Recent developments involving patch clamp have included very precise electrochemical imaging[14] and high throughput planar patch clamp methods.[15]

Because the gating described previously for biological ion channels is only thought to exist due to conformational changes, only a few studies have performed patch clamp on synthetic membranes, since no stochastic behavior would be expected for passive pores. These studies have shown anomalous fluctuations when patching onto track-etched membranes or flat PDMS surfaces, but the cause of these fluctuations in the absence of well-defined blocker molecules has not been satisfactorily addressed.[12,13,16,17] Proposed mechanisms for these fluctuations have included changes in surface charge at the pore wall,[16] thermal fluctuations that pinch off thin strands of water between the glass tip and PDMS,[12] and internal adsorption of ions which can result in chaotic behavior of ion concentration over time.[13]

In this work, we apply the patch clamp technique to study and understand ion transport through nanopores specifically patterned or otherwise in PDMS allowing for their character-

Received: September 16, 2012
Revised: February 18, 2013
Published: April 15, 2013

   dx.doi.org/10.1021/jp312659m | J. Phys. Chem. C 2013, 117, 9641−9651

ization. Anomalous events can occur in new situations that are entirely unexpected, so very thorough control experiments are necessary before making conclusions in any new platform. The observed fluctuations studied in this work are shown to be distinct from our recent observations[5,6] in single-walled carbon nanotube pores. In our recent carbon nanotube work, the duration of the fluctuations in the off state (the dwell time) is inversely related to the applied potential and varies with the type of cation in the system, indicating a well-defined, charged blocking event. In contrast, this work studies a mechanism that appears to be invariant with the applied electric field.

EXPERIMENTAL METHODS

We set up a patch clamp system using a Multiclamp 700B amplifier and Digidata 1440A digitizer from Molecular Devices. Glass pipets were freshly pulled before experiments using a Sutter pipet puller (Sutter P-1000) using 1.5 mm o.d. and 1.1 mm i.d. fire-polished borosilicate glass capillary tubing such that the inner tip diameter was 1.2 μm and a wall width of 170 nm, as verified by scanning electron microscopy (SEM). The tip and bath were filled with electrolyte solutions, and subsequent solutions were perfused through shielded polyethylene tubing using a syringe pump for infusion and an aspirator for withdrawal. The electrolyte solutions of a wide concentration range were prepared through serial dilution using Milli-Q deionized water. The entire setup was housed in a grounded Faraday cage. A detailed description of the setup can be found in the Supporting Information.

The PDMS surfaces were prepared using Sylgard 184 from Dow Corning. The base and curing agent were mixed in a ratio of 10:1 by mass, followed by 30 min of degassing under vacuum. The PDMS was then drop-cast onto a silicon chip and heat-cured on a hot plate at 180 °C for 15 min. Grooved PDMS surfaces were made using unwritten CD-R and DVD-R discs as templates using a procedure described in detail elsewhere.[18] AFM images showed CD-R templated PDMS had a groove depth of 73.1 ± 6.3 nm, with a groove spacing of 1.48 ± 0.03 μm; DVD-R templated PDMS had a groove depth of 75.8 ± 2.7 nm, with a grooved spacing of 0.73 ± 0.02 μm.

RESULTS AND DISCUSSION

Patch clamp experiments on both grooved and flat PDMS surfaces yielded stochastic current fluctuations, as shown in Figure 2. Current fluctuations were observed with solutions of LiCl, NaCl, KCl, CsCl, and $CaCl_2$ of concentrations ranging from 1×10^{-3} to 3 M. Persistent experimental artifacts were ruled out as the cause because these stochastic current fluctuations were observed in <30% of the flat PDMS samples and <50% of the grooved PDMS samples. PDMS samples were rinsed thoroughly with DI water and dried with nitrogen gas before patching onto them. AFM images generally showed a clean, flat surface so contamination is not thought to be an issue (see Figure S2 in the Supporting Information). Furthermore, the fluctuations disappear as the seal is tightened significantly past the point of a reasonable seal, indicating that electrical or grounding artifacts are not the cause. There are also no fluctuations observed when the pipet is just immersed in the bath solution, indicating that the patch itself is contributing to these fluctuations.

After patching onto the surface of flat PDMS samples and observing these fluctuations, many of them indicated the presence of a single pore (two Coulter states). To confirm that the conduction path in these cases exists within the PDMS itself,

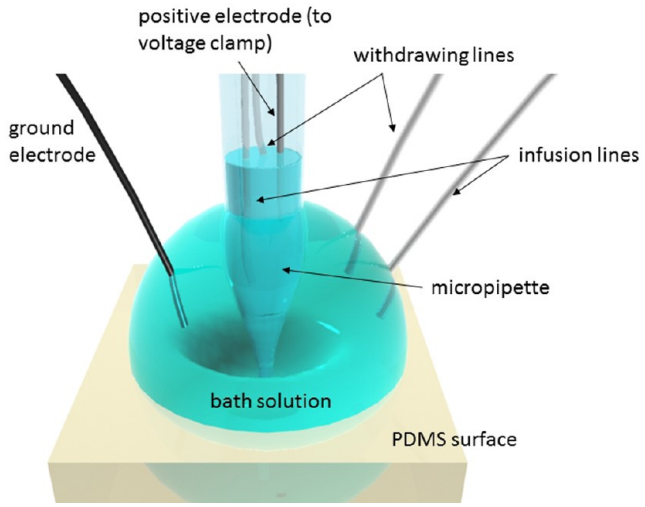

Figure 1. Schematic of patch clamp experiment on PDMS surface. The glass micropipet is pressed into the PDMS to form a seal between the solution in the tip and the bath. Infusion and withdrawing lines in the pipet tip and bath allow solution exchange on the same patched spot without affecting the seal.

grooved PDMS surfaces were made by templating PDMS using unwritten CD-R and DVD-R disks, which have tracks spaced 1.6 μm and 740 nm, respectively. Figure 3 shows an AFM image of a grooved PDMS surface made using a CD-R template, and outlines showing possible random placements of the tip onto the PDMS surface. Patching onto a grooved PDMS surface forms 0, 1, or 2 nanopores on the surface as shown. Overall, 16 out of 33 (48%) of grooved PDMS samples produced stochastic current fluctuations. In cases where no stochastic current fluctuations were observed, it is difficult to know whether a pore was formed or not since it is possible that the nanopore remains in a high conducting state or a low conducting state; this experiment can only distinguish the nanopore current from leakage current when there are fluctuations between the two conductivity states.

For example, two pores that switch conductivity states independently result in 3 or 4 current states. Three current states are observed when two independent pores are formed that have the same conductivity change when switching from an open to a closed state. Thus, the current state associated with a single pore being open is degenerate. Four current states are observed when two independent pores are formed which each have different conductivity changes when switching between open and closed states. Thus, there are two nondegenerate current states when a single pore is open and the other closed.

To further confirm that the pore was due to nanochannels made by the interface of PDMS and glass, the baseline and magnitude of stochastic current fluctuations were monitored as a function of tip penetration depth into the PDMS surface, as depicted in Figure 4. It should be noted that the distance of penetration was recorded from the stage micromanipulator, which is not an accurate measure of actual penetration depth since the pipet tip can be pushed back into its pipet holder. However, it is clear that the pore that is causing fluctuations can be compressed and made smaller, resulting in lower blockade currents. The baseline current is seen to go toward an asymptote around 25 pA, which may represent the inherent porosity of the PDMS substrate. This experiment confirms that the pore is due mainly to channels at the PDMS−glass interface rather than through defects in the glass, for example. Defects right at the

dx.doi.org/10.1021/jp312659m | J. Phys. Chem. C 2013, 117, 9641−9651

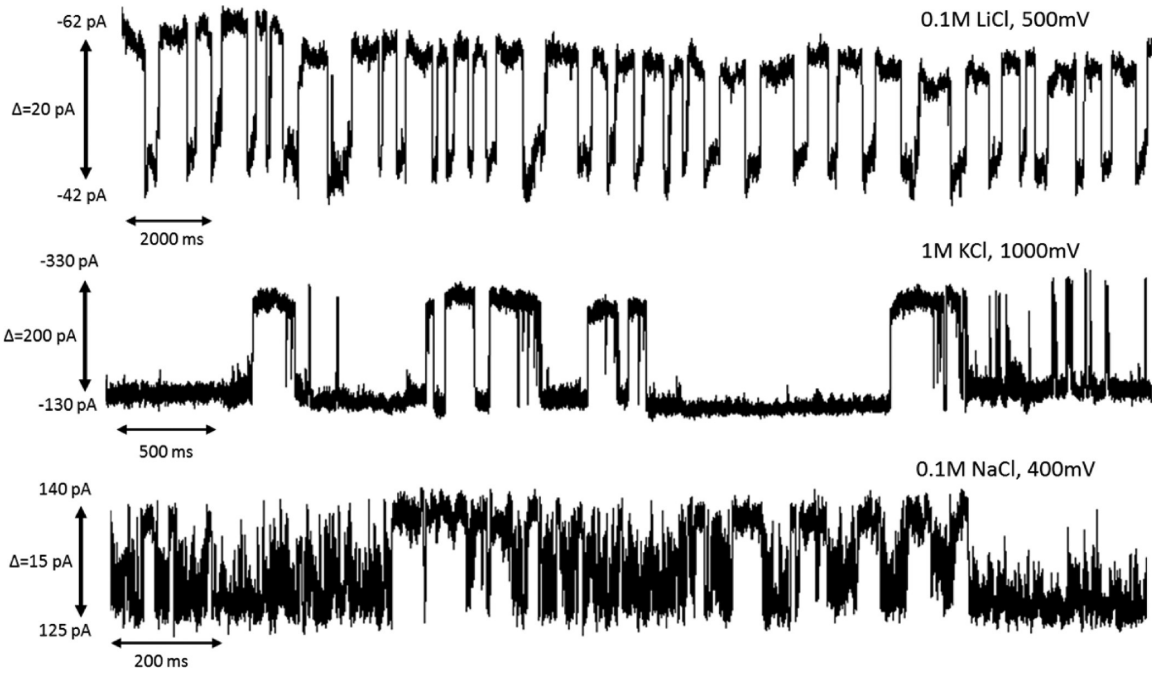

Figure 2. Representative current traces showing discrete stochastic current fluctuations when patch clamping onto flat PDMS surfaces. Negative currents imply a negative polarity being applied (the electrode inside the micropipet is at a negative bias with respect to the bath solution).

pipet tip could possibly contribute to forming part of the channel at the PDMS−glass interface, although SEM images of the tip show a surface smoother than that of the grooved PDMS samples (see Figure S1), making this possibility unlikely. While PDMS is known to be an inherently porous material for gases and liquids,[19,20] which would contribute slightly to the leakage current, the diffusive transport of electrolyte through the free volume of the polymer is not expected to give rise to clear, discrete current states. On the other hand, pores formed at the grooved PDMS−glass interface have a much likelier possibility of forming discrete, straight-line pores that could be individually blocked.

Unlike previous work in our group studying stochastic pore-blocking from ions in single-walled carbon nanotubes (SWNT), where the majority charge carriers were found to be protons,[5,6] concentration experiments confirmed that the majority carriers in these PDMS nanochannels were the electrolyte cations and anions (see Figure 4c,d).

The relationship between pore diameter and conductivity can be obtained using full molecular dynamics (MD) simulations which can be very computationally intensive.[21] Another method employs a multiscale approach—using MD simulations to generate ion mobilities inside the nanopore and continuum models (Navier−Stokes and Poisson−Nernst−Planck equations) to simulate the electrohydrodynamics.[22] These sophisticated models are most necessary when the pore diameter is <1 nm, and the Debye length is comparable with the pore radius.[21,22] In this case, where the pore geometry is less well-defined and diameter unknown beforehand, simpler analyses are carried out to give a rough estimate of effective pore diameters.

A simple model relating pore conductance with the effective pore diameter, assuming a cylindrical pore geometry and a charged layer of zero thickness adjacent to the oppositely charged surface (similar to the Helmholtz double layer approximation of zero thickness), is provided by eq 1,[23] which shows that the pore conductance is

$$G = \frac{\pi}{4}\frac{{d_{\text{pore}}}^2}{L_{\text{pore}}}\left((\mu_+ + \mu_-)n_{\text{electrolyte}}e + \mu_K\frac{4\sigma}{d_{\text{pore}}}\right) \quad (1)$$

where G is the pore conductance (A/V), d_{pore} is the diameter of the pore (m), L_{pore} is the length of the pore (m), μ_+ and μ_- are the ion mobilities of the cation and anion, respectively ($m^2/(V\ s)$), $n_{\text{electrolyte}}$ is the number density of the electrolyte species (no./m^3), e is the elementary charge (1.602×10^{-19} C), and σ is the negative surface charge density of the nanopore (C/m^2). The Supporting Information provides calculations that show a relatively weak surface charge of roughly -0.015 C/m^2 (or 11 nm^2/e^-) for native PDMS. The length of the pore can be assumed to be the thickness of the micropipet tip (170 nm).

A second relationship that better accounts for the diffuse double layer of finite thickness inside the nanopore is

$$G = \frac{\pi}{4}\frac{(d_{\text{pore}} - 2\kappa_D)^2}{L_{\text{pore}}}\left((\mu_+ + \mu_-)n_{\text{electrolyte}}e + \mu_K\frac{4\sigma d_{\text{pore}}}{(d_{\text{pore}} - 2\kappa_D)^2}\right) \quad (2)$$

which assumes that within the Debye length (κ_D (nm) = 0.304/$(I(M))^{1/2}$) from the negatively charged pore walls there is a concentration of cations that cancels out the surface charge (assuming anion concentration is negligible in this region); outside of this diffuse double layer is the bulk ion concentration.

Third, if the mechanism of blocking is due to a phase transition, as will be postulated later, the fractional change of mean ion density inside the nanopore relative to the bulk ion density, denoted Δk, is only about 0.15.[24] As the mean ion density accounts for variation due to the charged surfaces, the surface charge term is not needed, and eq 3 can be used to represent the change in conductance between the high- and low-conducting states. This calculation results in a larger calculated diameter since a larger nanopore is required to produce the same

dx.doi.org/10.1021/jp312659m | J. Phys. Chem. C 2013, 117, 9641−9651

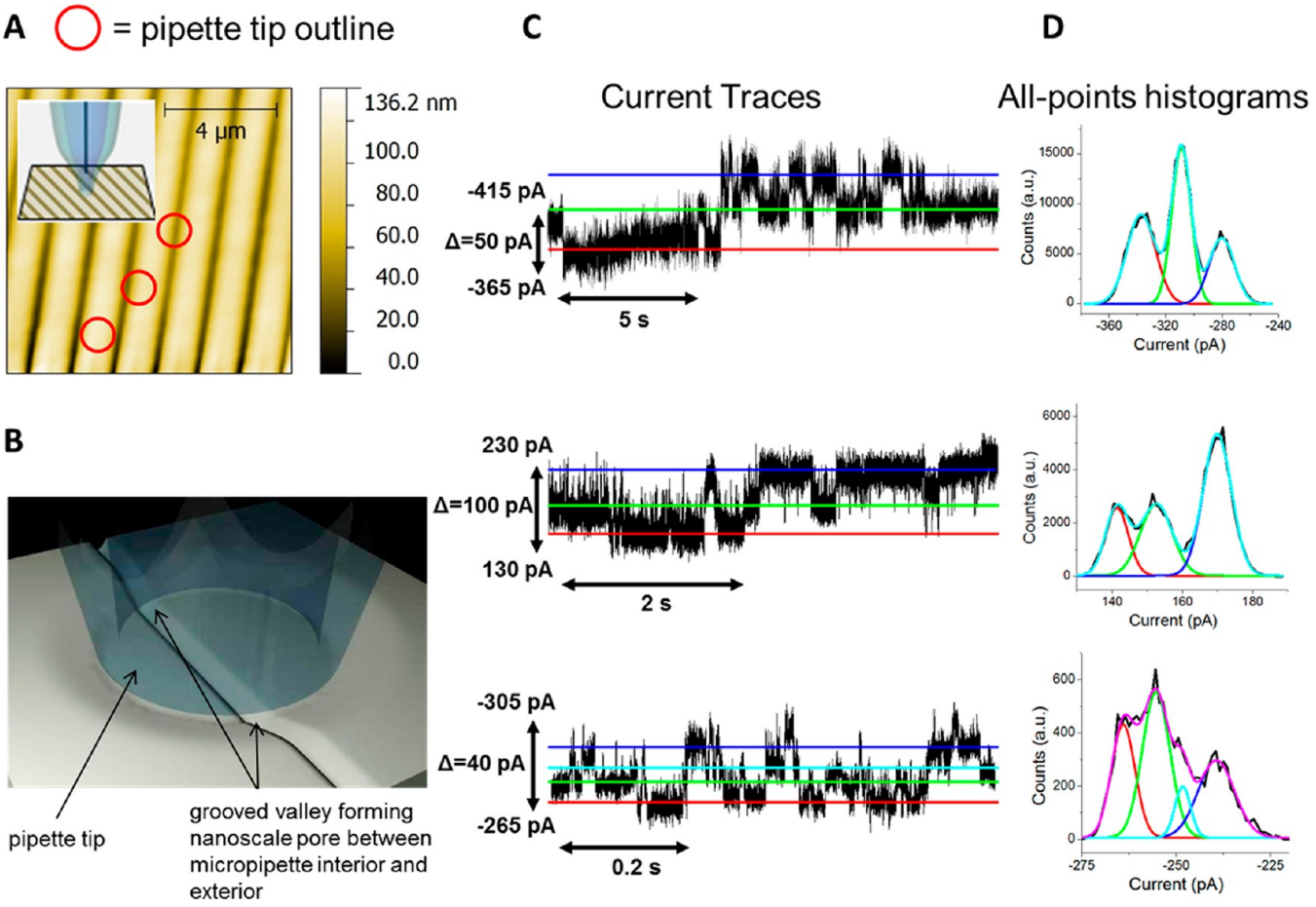

Figure 3. Patch clamp on grooved PDMS surfaces. (A) An AFM image of PDMS grooves formed using a CD-R disk as a master. The red circle depicts the outline of a 1.2 um diameter pipet tip, and random placements on the surface will yield preferentially 0−2 expected channels between the glass tip and PDMS surface. (B) A schematic of patching onto a grooved PDMS surface preferentially forming 2 nanopores. (C) Current traces from patching onto grooved surfaces using 0.1 M NaCl demonstrate that 3 or 4 Coulter states appear, indicating the presence of two channels. (D) The all-points histograms verify the presence of multiple states.

conductivity change if the density change is a fraction of that of the bulk.

$$\Delta G = \frac{\pi}{4}\frac{d_{\text{pore}}^{2}}{L_{\text{pore}}}((\mu_{+} + \mu_{-})(\Delta k)n_{\text{electrolyte}}e) \quad (3)$$

The diameters for 10 samples were calculated using these three methods. The first two methods assume that the pore is completely empty in the low-conducting state and so G is replaced by ΔG, the total change in conductance between the two states as determined by the blockade current. Figure 5 shows the diameter distributions using these different calculation methods. In the first case, the diameters range from 0.6 to 3.2 nm (1.9 ± 0.7 nm); the second case yields diameters from 0.8 to 4.6 nm (2.8 ± 1.1 nm); the third case yields diameters from 3.6 to 11.2 nm (7.4 ± 2.1 nm). In all cases, the pore diameter is on the order of several nanometers. However, it is not possible to characterize the pores directly because their existence depends on the contact of the patch clamp tip with the PDMS surface.

To further confirm the presence of nanometer-sized, hydrophobic pores, experiments were performed using anionic and nonionic surfactants. The results, shown in Figure 6a, demonstrate that increasing concentrations of sodium dodecyl sulfate (SDS), an anionic surfactant, leads to an increase in baseline conductance. The same concentration experiment with Triton X-100, a nonionic surfactant with only polar head groups, shows the opposite trend of decreasing conductance. In both cases, the baseline conductance flattens out past the critical micelle concentration (cmc). The cmc represents the point at which adding more surfactant results in mostly forming micelles. Assuming there is equilibrium between free monomer surfactant in bulk solution and adsorption inside the nanopore, one would expect any effect of surfactant concentration on nanopore transport would diminish past the cmc, which is indeed observed.

Assuming the pore is hydrophobic, the aliphatic part of the surfactant molecule will to adsorb to the hydrophobic pore surface. For a nonionic surfactant, surface adsorption will only decrease the cross-sectional area of the pore in theory and result in lower pore conductance. However, a significant decrease in pore conductance only occurs if the pore diameter is small, commensurate in scale with the thickness of the adsorbed layer. Assuming that the entire baseline current moves through approximately a single pore and Triton X-100 (~2 nm in length) coats uniformly around a cylindrical pore, the original pore diameter is calculated to be about 6.7 nm. However, if the pore is slit-shaped, the calculated pore height is around 4.8 nm. These estimates agree closely with those made directly from the pore conductance equations in the previous section.

dx.doi.org/10.1021/jp312659m | J. Phys. Chem. C 2013, 117, 9641−9651

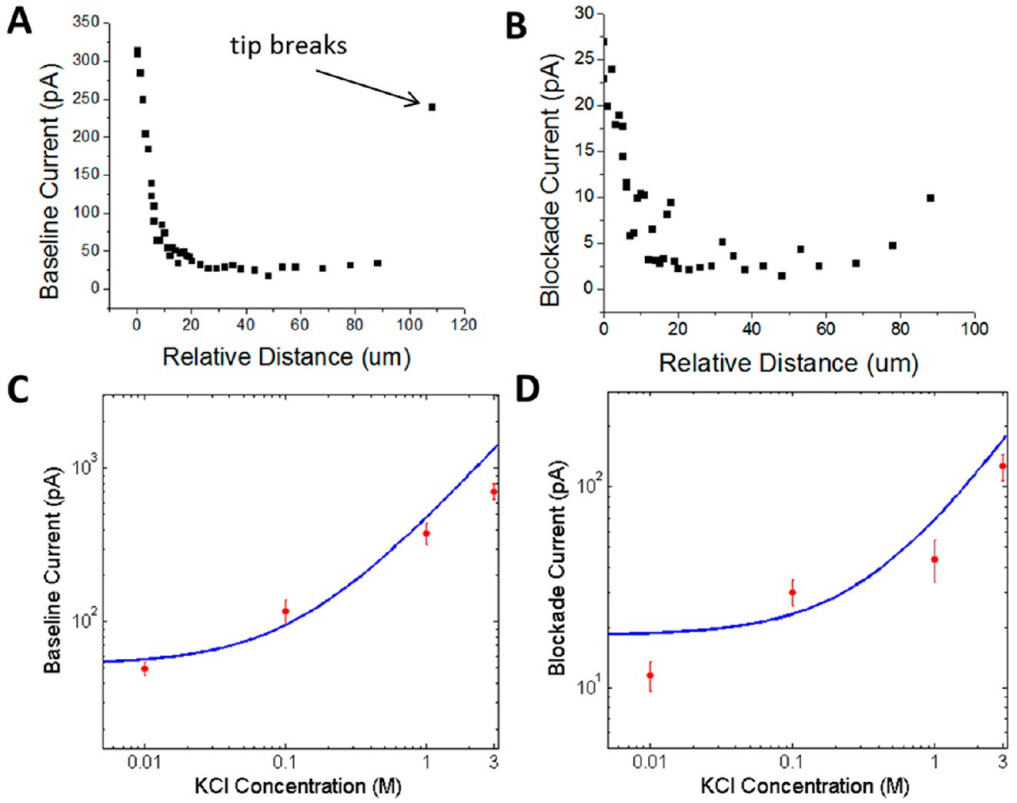

Figure 4. Effect of tip compression into the PDMS surface is to decrease the overall baseline current (A) and blockade current (B) indicating the pore is due to the PDMS, which is deformable under pressure. If too much pressure is applied, the pipet tip begins to crack, resulting in a higher baseline current. The identity of the majority charge carriers can be seen by observing the baseline conductance (C) and blockade current (D) as a function of electrolyte concentration. It is clear that the baseline and blocked current are carried by the electrolyte. The blue line is a fit to the data using eq 1.

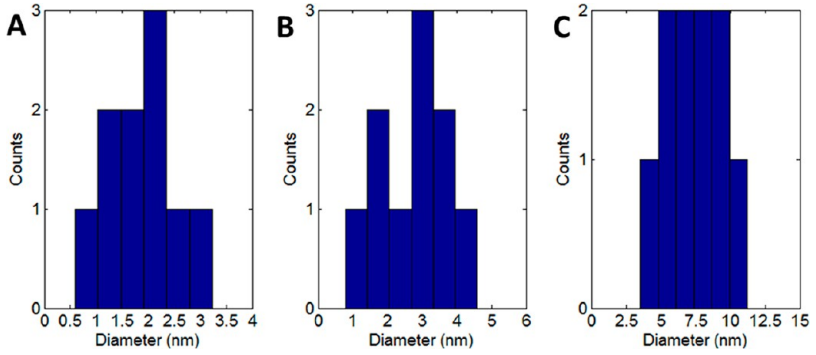

Figure 5. Calculated diameter distributions under the same experimental conditions (0.1 M NaCl, 1000 mV, grooved PDMS sample, 170 nm thick tips). The diameters are calculated (A) using eq 1, (B) using eq 2, and (C) using eq 3.

$$\frac{G}{G_{surf}} = \frac{0.09\ \text{nS}}{0.015\ \text{nS}} = 6 = \frac{d^2}{{d_{surf}}^2} = \frac{d^2}{(d - \Delta d)^2} = \frac{d^2}{(d - 2(2\ \text{nm}))^2} \rightarrow d = 6.7\ \text{nm} \quad (4)$$

$$\frac{G}{G_{surf}} = \frac{0.09\ \text{nS}}{0.015\ \text{nS}} = 6 = \frac{h}{h_{surf}} = \frac{h}{h - \Delta h} = \frac{h}{h - 2(2\ \text{nm})} \rightarrow h = 4.8\ \text{nm} \quad (5)$$

For an anionic surfactant, like SDS, the pore surface will become more charged, which will significantly enhance transport only if the pore is small (the surface transport term in eq 1 is inversely proportional to diameter). There are two competing effects upon addition of SDS surfactant: the pore diameter will decrease which reduces bulk transport, but the surface charge will increase which enhances surface transport. The Supporting Information provides a calculation showing that for a 6.7 nm diameter pore the observed overall increase in conductance upon addition of SDS can be achieved with a physically reasonable surface charge density (0.28 C/m^2 or 0.57 nm^2/e$^-$) which is provided by the surfactant molecules.

There have been several studies performing voltage clamp on nonbiological nanopores that observe stochastic current fluctuations or resistive pulses. There have been several mechanisms proposed to explain these discrete fluctuations, all of which may be accurate for the specific system in study: blockage by a charged ion or molecule,[5−7,23] nanoprecipitation,[25]

dx.doi.org/10.1021/jp312659m | J. Phys. Chem. C 2013, 117, 9641−9651

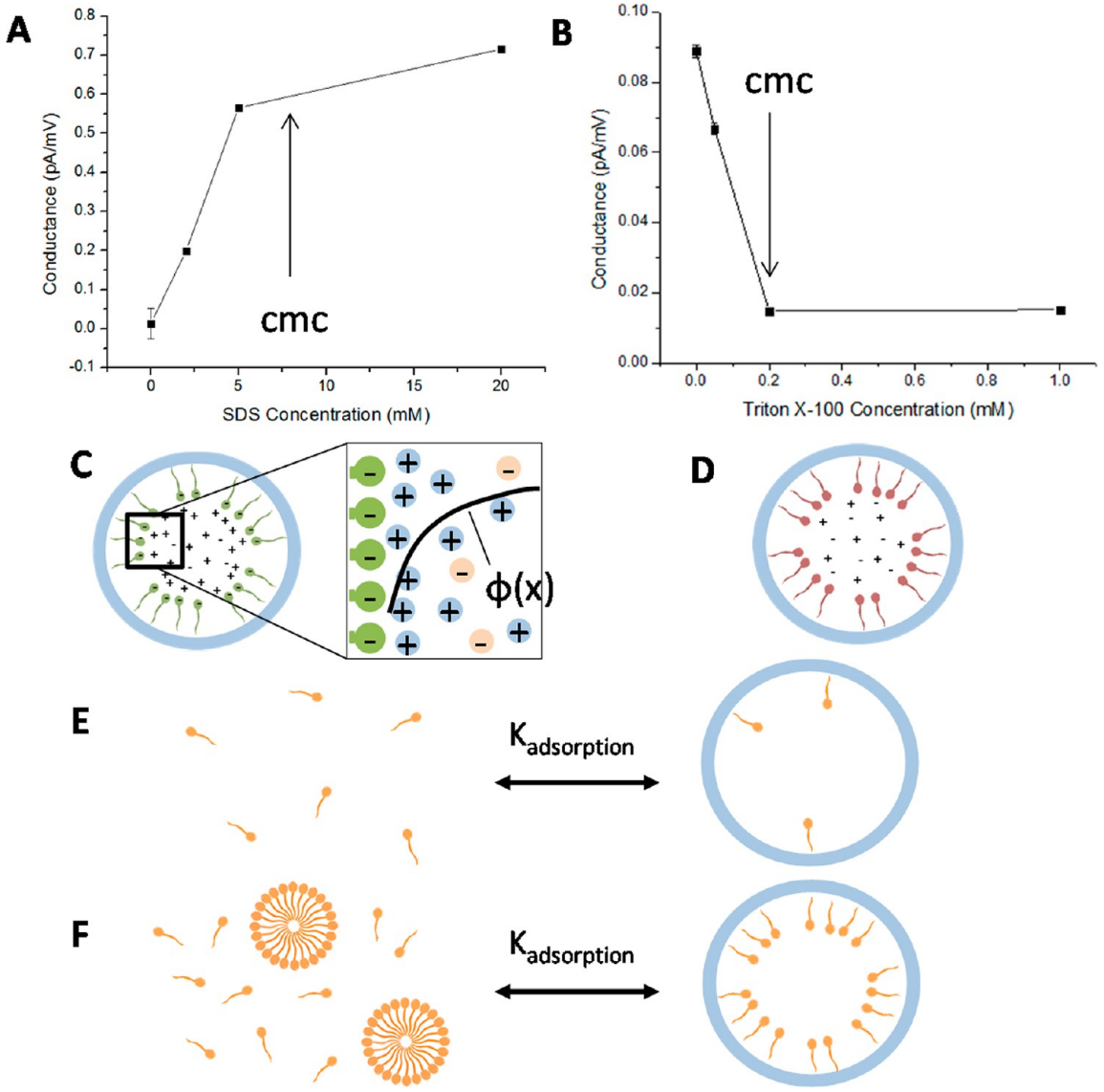

Figure 6. Effect of surfactant on pore properties. (A) The conductance increases upon addition of anionic SDS surfactant, and the change in conductance decreases as the concentration increases past the critical micelle concentration (cmc). (C) As shown in the schematic, an increase in pore conductance can be attributed to the increase in surface charge transport due to the presence of charged groups inside the pores which causes a buildup of charge near the surface. $\varphi(x)$ is the electric potential near the surface. (B) The conductance decreases upon addition of nonionic Triton X-100 surfactant, and this change flattens out past the cmc. (D) The schematic shows that adsorption of nonionic surfactant does not increase surface charge transport but only serves to occlude the pore area. (E) When the surfactant concentration is below the cmc, increasing the surfactant concentration increases the amount of free monomer in solution, which will increase the surfactant adsorption into the PDMS nanopores. (D) Past the cmc, increasing surfactant in solution serves mainly to increase micelle concentration. Thus, the PDMS nanopore becomes saturated with surfactant molecules past the cmc.

and complete wetting/dewetting of the nanopore (e.g., the presence of a nanobubble).[8,22]

To ensure that the observed stochastic current fluctuations are not due to nanoprecipitation effects inside the PDMS nanopore, precipitation was forced to occur by adding $CaCl_2$ on one side and KH_2PO_4 on the other side. A similar experiment by Powell et al.[8] demonstrated stochastic current fluctuations in track-etched PET membranes due to transient precipitates blocking the pore, followed by redissolution caused by the applied voltage. In our experiment, an electrical bias was applied such that calcium and phosphate ions would be driven toward the nanopore and precipitate to form $CaHPO_4$. As Figure 7 shows, prior to addition of KH_2PO_4 to the bath side, there were no fluctuations observed. However, once KH_2PO_4 was added, there were immediate stochastic current fluctuations that were more asymmetric and triangular-shaped compared to typical current traces observed when just simple electrolytes (e.g., KCl or NaCl) are used, as shown in Figure 2. This asymmetry is in agreement with previous observations of nanoprecipitation.[25] Hence, the mechanism responsible for the current fluctuations that is the focus of this work is distinct from nanoprecipitation.

Stochastic pore blocking of the nanopore by the ions themselves was ruled out since the blockade current increases with electrolyte concentration, showing that the ions are the majority charge carriers. Also, pore blocking was not observed in the presence of larger charged molecules, such as DNA, ruling out blocking by a molecule passing through the pore. To further distinguish between blockage by any charged species (the

dx.doi.org/10.1021/jp312659m | J. Phys. Chem. C 2013, 117, 9641−9651

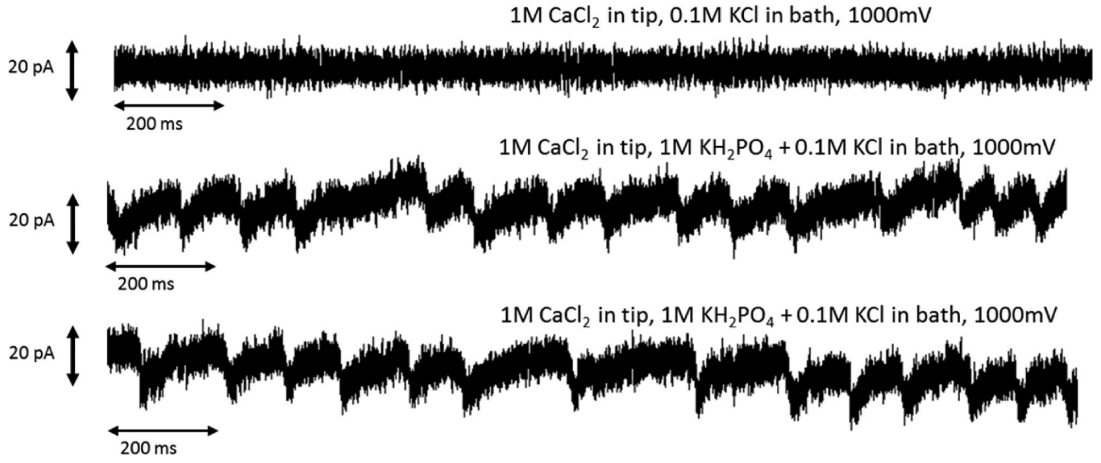

Figure 7. Experimental results demonstrating nanoprecipitation-induced current fluctuations inside the nanopore formed by the tip and PDMS surface. With $CaCl_2$ in the tip and only KCl in the bath, no stochastic fluctuations were observed. However, once KH_2PO_4 was added, this would precipitate to $CaHPO_4$ when the phosphate anion combines with the calcium cation on the other side. The current fluctuations are asymmetric and sloped. The nanoprecipitation-induced fluctuations in PDMS nanopores shown here are quite different than the fluctuations observed using normal electrolytes (e.g., NaCl and KCl), thus ruling out nanoprecipitation as the cause for stochastic current fluctuations.

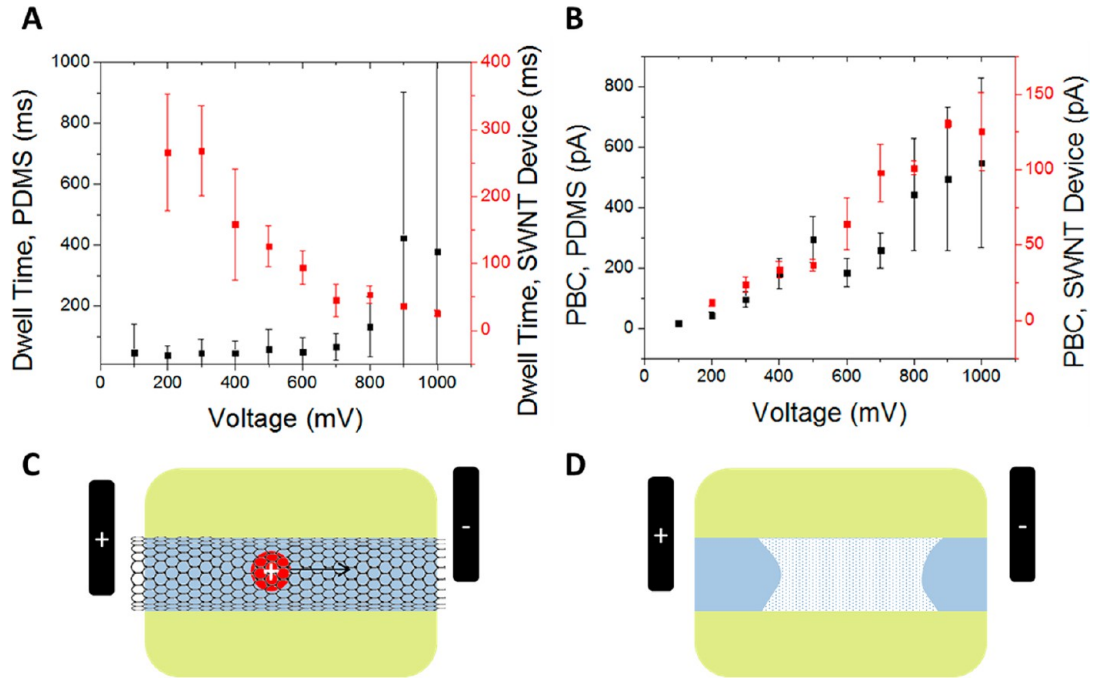

Figure 8. Comparison of the discrete, stochastic current fluctuations of PDMS nanopores and SWNT nanopores. (A) Dwell times as a function of voltage for PDMS nanopores (black, left axis) and for SWNT nanopores (red, right axis). While the dwell times are inversely related to the applied voltage for the SWNT nanopore, they are relatively invariant with respect to voltage for the PDMS nanopore. The large error bars in the PDMS case are due to groups of fluctuations located fewer and farther between at higher voltages. (B) Pore-blocking currents (PBC) as a function of voltage for PDMS nanopores (black, left axis) and for SWNT nanopores (red, right axis). In both cases, there is a roughly linear scaling of PBC with applied voltage. The PDMS nanopore data were taken using 0.1 M NaCl, and the SWNT nanopore data were taken using 1 M $CaCl_2$. The inverse relationship of dwell times with applied voltage corresponds to a charged blocker moving through the pore (C), while having dwell times invariant with applied voltage is indicative of an uncharged blocker, which could be present as a vapor phase inside of the pore (D). The linear relationship between the PBC and applied voltage in both cases indicates that the blocked current is carried by charged species. These charged species are believed to be protons in the SWNT nanopore case[5] and electrolyte ions in the PDMS case.

Coulter effect) and a phase transition, the blockade currents and dwell times were tabulated as a function of applied voltage in Figure 8. Pore-blocking data were collected and analyzed from devices made using our previous platform for studying transport through single-walled carbon nanotubes—the blocking phenomenon in these cases was confirmed to be caused by ions blocking an otherwise stable proton current.[5] This blocking mechanism involves a charged blocker moving through the pore, interrupting a baseline current carried by charged particles resulting in a dwell time that decreases as a function of the applied voltage and a pore-blocking current that scales linearly with the applied voltage. As with SWNT nanopores, the PDMS nanopores also demonstrated pore-blocking currents that increase linearly with applied voltage. However, the PDMS nanopores showed a widely

dx.doi.org/10.1021/jp312659m | J. Phys. Chem. C 2013, 117, 9641−9651

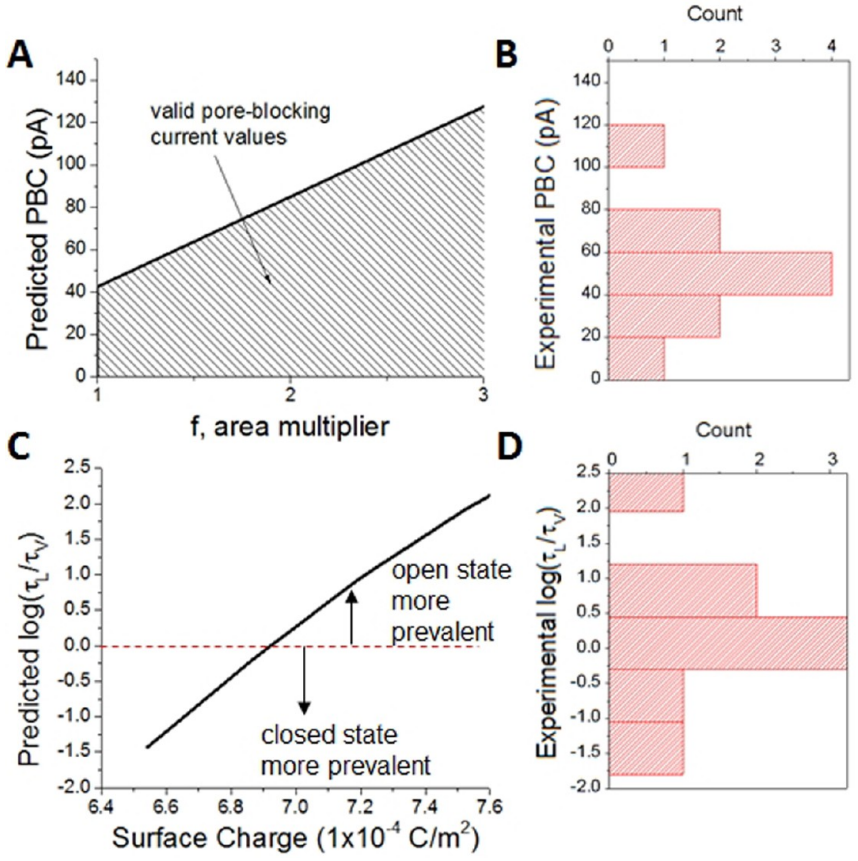

Figure 9. (A) Predicted log of the ratio of residence times in the liquid and vapor states versus area factor accounting for deviation from a cylindrical pore model according to the model proposed by Palmeri et al.[24] (B) The wide range of possible residence time ratios is reflected in the experimental data, where if fluctuations are observed, there is a wide range of residence time ratios. (C) The model also predicts an envelope of pore-blocking currents (PBC), which varies depending on the deviation from a circular pore cross section. (D) The experimental pore-blocking currents fall within this envelope for $f < 3$.

variable dwell time distribution that was not affected by the applied voltage. We conclude that the current blocker is uncharged and therefore not affected by the electric field in the pore.

These results suggest an uncharged "blocker" with a baseline current carried by ions. We explored the theory that there is a phase transition occurring inside the nanopore which causes an ionic concentration change inside the nanopore, such that the pore is rendered nonconducting due to water vapor blocking the pore. This mechanism has been studied theoretically for short hydrophobic/weakly charged nanopores[24,26,27] and observed experimentally in track-etched PET nanopores with the interior functionalized with hydrophobic groups.[8] This work provides further evidence that this phenomenon is occurring by demonstrating that dwell times are invariant with applied voltage.

To further confirm the existence of a phase transition as the cause of stochastic current fluctuations, we sought out a theory from the literature that offered predictive estimates of the pore-blocking currents and dwell times. Palmeri et al.[24] have developed a model using variational field theory that predicts phase transitions to occur for electrolyte solutions confined to neutral and weakly charged cylindrical nanopores. Their model considers the diameter of the pore, the dielectric constants of the solution and pore walls, surface charge on the pore walls, the effective Donnan potential inside the pore, and bulk ionic concentration. The major assumptions of Palmeri's model are as follows: (1) a perfectly cylindrical pore surface, (2) uniform surface charge density, (3) constant electrostatic potential inside the pore, and (4) no steric effects of ions (ions act as point charges). In reality, the pores studied here are noncylindrical, may not have uniform charge density along the length of the pore, the electrostatic potential is not constant as we are applying a voltage across the pore, and ion size may indeed have significant effects at the nanoscale; thus, while we can compare experiment and theory, one would not expect numerically equivalent results. Their model predicts that at low enough pore diameters there exists a bulk electrolyte concentration around which the partition coefficient exhibits an abrupt change, where the partition coefficient is defined as $k = \langle\rho\rangle/\rho_b$, where $\langle\rho\rangle$ is the average ionic concentration inside the pore (mol/L) and ρ_b is the bulk ionic concentration (mol/L). Thus, there exists a high conductivity liquid (L) phase and a low conductivity vapor (V) phase. If the stochastic current fluctuations are due to fluctuating between these V and L phases, the difference in partition coefficients provides a way to estimate the magnitude of pore-blocking currents, given an applied voltage and pore length, using

$$\langle\rho\rangle = \rho_b(k_L - k_V) \tag{6}$$

$$\Delta I = I_+ + I_- = (J_+ + J_-)A = q\langle\rho\rangle v_{avg}A = q\langle\rho\rangle(\mu_+ + \mu_-)EA \tag{7}$$

$$\Delta I = q\rho_b(k_L - k_V)(\mu_+ + \mu_-)\frac{\Delta V}{L}A \tag{8}$$

dx.doi.org/10.1021/jp312659m | J. Phys. Chem. C 2013, 117, 9641−9651

where k_L and k_V are the partition coefficients of the liquid and vapor phases, respectively, ΔI is the predicted pore-blocking current (A), I_+ and I_- are the currents associated with positive and negative ions (A), J_+ and J_- are the current densities (A/m^2), A is the pore cross-sectional area (m^2), v_{avg} is the average velocity of the ions (m/s), μ_+ and μ_- are the ion mobilities of the cations and anions, respectively (m^2/(V s)), E is the electric field across the pore (V/m), ΔV is the voltage applied across the pore (V), and L is the length of the pore (m). The area of the pore is given by

$$A = f\pi a^2 \tag{9}$$

where a is the radius of the nanopore (m) and f is some factor that accounts for the noncylindrical shape of the pore which is unknown. It is possible that the pore may be a wide slit-shaped pore, for example. The model predicts a difference in partition coefficients, Δk, roughly from 0 to 0.15 for neutral nanopores, which changes slightly depending on the bulk concentration, pore diameter, and surface charge. The diameter distribution of samples tested for this study were presented earlier in Figure 5B, assuming a cylindrical pore ($f = 1$) and $\Delta k = 0.15$.

To compare with our experiments, we used $\rho_b = 0.1$ M, $a = 1$ nm, $\mu_+ = \mu_{Na^+} = 51.9 \times 10^{-9}$ m^2/(V s), $\mu_+ = \mu_{Cl^-} = 79.1 \times 10^{-9}$ m^2/(V s), $\Delta V = 1.0$ V, and $L = 170$ nm to get an envelope of predicted pore-blocking currents. The predicted pore-blocking current has a maximum value around 40−120 pA depending on the value of f used, where f is a factor accounting for noncircular pore cross sections ($f = 1$ for circular cross section). In Figure 9A,B, we compared these predicted pore-blocking currents with experiments made under similar conditions ($\rho_b = 0.1$ M NaCl, $\Delta V = 1.0$ V, and $L = 170$ nm) and find very good agreement for low values of $f < 3$.

The model also predicts the thermodynamic stability of each phase in a region of coexistence. Over small differences in surface charge, there is predicted to be a wide range of ratios of residence times (τ_L/τ_V), that is, the time spent in the high-conducting state versus the time spent in the low-conducting state. For the particular example presented in their study ($\rho_b = 1$ mol/L, $a = 0.617$ nm), it was predicted that as the surface charge varied from 6.5×10^{-4} to 7.5×10^{-4} C/m^2, the τ_L/τ_V varied roughly from 0.01 to 100, thus showing that slight deviations in surface charge, keeping ionic concentration and diameter constant, can result in significant changes in these residence time ratios. The surface charge explored in Palmeri's study is very weak (roughly 1 charge per 230 nm^2), although within the same vicinity as the surface charge for the PDMS surfaces (roughly 1 charge per 10−20 nm^2). We assume that whenever the conditions (diameter, concentration, and surface charge) are such that fluctuations between a high- and low-conducting state are observed, slight deviations in any of these parameters will also result in significant sample-to-sample variation in the ratios of residence times similar to the specific case ($\rho_b = 1$ mol/L, $a = 0.617$ nm, $\sigma = (6.5-7.5) \times 10^{-4}$ C/m^2) studied by Palmeri et al.[24] It could be expected that among the samples that do demonstrate stochastic current fluctuations, there will be a distribution of actual surface charge values for each patch area so that one would expect to sample from the wide range of possible residence time ratios. Figure 9 shows that experimentally the high-conducting state can occur more often or less often by factors as high as 25, in line with the qualitative predictions by the model. It should be noted that at very high or very low τ_L/τ_V ratios, it would be difficult to realize that rare stochastic current fluctuations were actually occurring as opposed to random, rare noise artifacts. In summary, the comparisons of pore-blocking currents and residence time ratios with the model proposed by Palmeri et al.,[25] along with dwell times that are invariant with applied voltage, provide evidence that the observed stochastic current fluctuations are due to switching between high-conducting liquid and low-conducting vapor phases.

However, it is acknowledged that there are some possible drawbacks of applying this model to the PDMS nanopores. For example, the model considers a pore in thermal and chemical equilibrium with the bulk, and it is assumed in the model derivation that the Donnan potential is constant within the pore. However, the applied voltage ensures that the system is not in equilibrium and the potential across the pore is not uniformly varying. It is unclear if the qualitative results of the model hold under these conditions. Furthermore, the model predicts that the bulk concentration at which phase coexistence occurs varies inversely with the pore radius. Thus, one would expect that if the pore diameter remains constant, there would be only one bulk concentration where fluctuations are observed; in actuality, there is a wide range of ionic concentrations where fluctuations are observed for a single patch. It is possible that the pore geometry is noncylindrical, resulting in different sections of the pore of varying dimensions which are active depending on the bulk concentration. Further experiments with well-defined pores and surface charge are needed to more completely confirm the existence of liquid/vapor transitions as the cause of stochastic fluctuations in these types of pores.

Experiments varying the temperature of the system were performed to confirm whether a phase transition was occurring, but the results were inconclusive; detailed results of these experiments are provided in the Supporting Information. Theories that assert that stochastic fluctuations occur at the phase boundary between high and low conducting states as a first-order transition suggest that increasing the temperature and keeping all other parameters constant should halt the fluctuations. As one moves into the single phase region, for example, either the high or low conductance state should persist. However, stochastic events were observed as the temperature was steadily ramped from room temperature up to 42−62 °C in three trials; eight other trials showed no events at all through the temperature increase. In one case, the events disappeared above 60 °C, although this occurred just before the bath solution evaporated. The other two cases did not go above 42 and 57 °C, and events persisted from room temperature through the maximum temperature. As shown in the Supporting Information, the pore-blocking current is not well-correlated with temperature. This may be due to the fact that changing temperature has other effects such as changing the pore size, solution viscosity, solution concentration through evaporation, surface charge, etc. It is possible that as the temperature changes, the changing pore geometry and solution conditions allow it to remain on or otherwise traverse the phase coexistence curve. Carefully controlled temperature experiments will be needed to fully verify the presence of phase transitions in these systems.

In attempts to further characterize the shape of these PDMS nanopores, we introduced $[Ru(bpy)_3]^{2+}$ (1.2 nm in diameter) to the system. Among other uses, this molecule is often employed as a probe molecule for transport measurements to determine steric selectivity in pores commensurate in size to its diameter. However, upon addition of this molecule in concentrations $>5 \times 10^{-8}$ M there is reduction in overall conductance, and for concentrations $>1 \times 10^{-4}$ M, there is complete shutdown of any ionic transport even though relatively high concentrations of

dx.doi.org/10.1021/jp312659m | J. Phys. Chem. C 2013, 117, 9641−9651

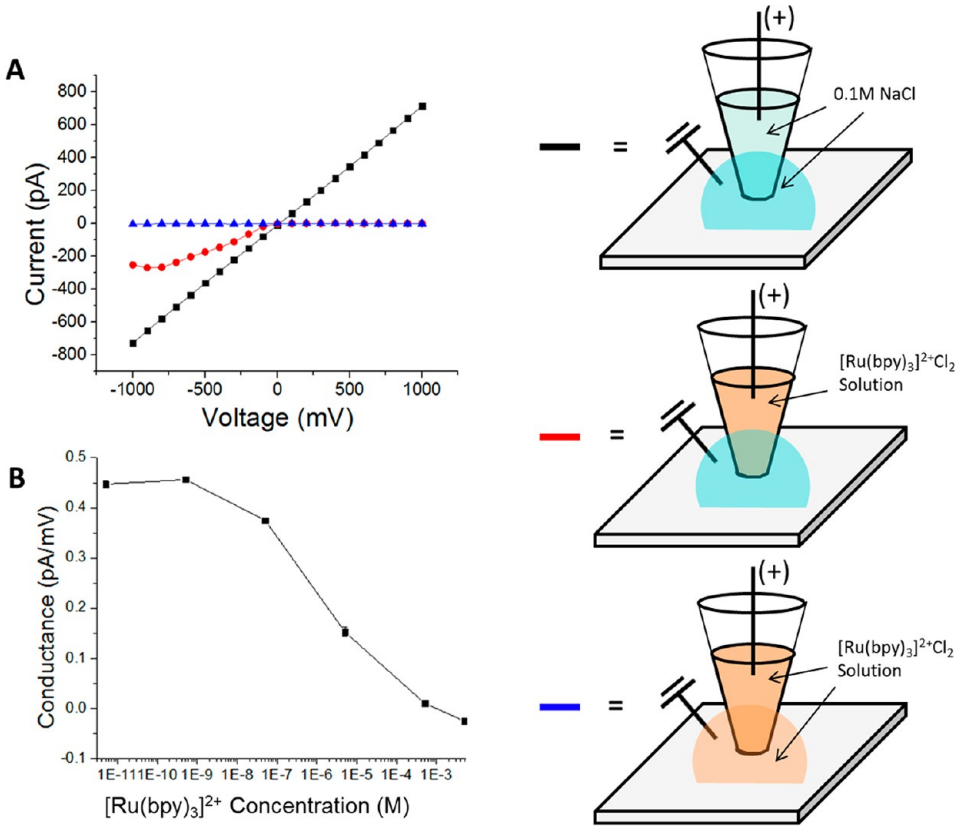

Figure 10. (A) Experimental *IV* curves showing that a simple electrolyte solution (0.1 M NaCl) in the pipet tip and bath results in a linear *IV* curve, while addition of 50 mM $[Ru(bpy)_3]^{2+}$ to the salt solution to one side of the bath causes complete current shutdown when the polarity is such that the $[Ru(bpy)_3]^{2+}$ ion is driven toward the pore, and complete current blockage is observed when $[Ru(bpy)_3]^{2+}$ is added to the salt solution on both sides at sufficient concentrations. (B) The overall conductance as a function of $[Ru(bpy)_3]^{2+}$ concentration. Conductance begins to decrease starting at 5×10^{-8} M $[Ru(bpy)_3]^{2+}$. Hence, the absence of conductance of this organometallic ion is not, itself, proof of steric rejection from a hydrophobic nanopore.

NaCl (0.1M) still exist in the pipet tip and bath, as Figure 10 demonstrates. If $[Ru(bpy)_3]^{2+}$ is added to just one side, we find a shutdown of both pore and leakage conductances if the polarity of the applied voltage is such that the $[Ru(bpy)_3]^{2+}$ ion is driven toward the pipet tip/PDMS interface containing the nanopores. These results strongly suggest that for relatively hydrophobic pores of nanometer-sized dimensions, one can have $[Ru(bpy)_3]^{2+}$ physisorbed on the interior of the pore, thus blocking overall transport. Further experiments performed demonstrated the reversibility and reproducibility of this $[Ru(bpy)_3]^{2+}$ physisorption.

The model proposed by Palmeri suggests that the presence of divalent cations would decrease the negative surface charge inside of the pore, which would cause the nanopore to switch from a high-conducting to a low-conducting state. As mentioned before, Palmeri's model assumes ions behave as point charges, with only Coulombic interactions present between ions. $[Ru(bpy)_3]^{2+}$, however, is ~1.2 nm in diameter, and thus it cannot shield surface charge as effectively as Mg^{2+}, for example. Furthermore, there are significant van der Waals and dipole–dipole interactions present in $[Ru(bpy)_3]^{2+}$ that are not accounted for by the model. From our observations, it seems most likely that this ruthenium complex is adsorbing onto the inside of the pore, and at sufficient concentrations, completely blocks current through the pore. The conclusion from this set of experiments is that careful analysis is needed to ensure that transport results using probe molecules such as $[Ru(bpy)_3]^{2+}$ are not due to pore blockage caused by condensation and physisorption, especially in nanometer-scale hydrophobic pores.

CONCLUSIONS

To summarize, we study a unique, stochastic phenomenon in both grooved and flat PDMS substrates that would not be expected to have any analogue to biological ion channels for which patch clamp techniques are normally used. This phenomenon was studied in depth to show the presence of nanopores formed at the interface of PDMS and glass when a patch is formed which imparts deformable properties to the pore. Transport through PDMS nanopores was confirmed by observing reproducible, multiple current states when patching onto grooved PDMS surfaces. The mechanism for these fluctuations is compared to Coulter blocking by ions in single-walled carbon nanotubes and nanoprecipitation, showing that the mechanism is fundamentally different. We compared our results with a model in the literature that predicts the coexistence of two phases at normal experimental conditions. Comparisons of the pore-blocking currents and residence time ratios with the model, along with the invariant nature of dwell times with applied voltage, suggest the plausibility of the mechanism being stochastic phase transitions inside the nanopore. Furthermore, the estimated pore diameter (ranging from 0.6 to 11.2 nm, depending on the calculation method) and surface charge (-0.015 C/m^2) are in line with those considered by the proposed model. In this study we have demonstrated a simple method for creating deformable, interfacial nanopores, with a

dx.doi.org/10.1021/jp312659m | J. Phys. Chem. C 2013, 117, 9641–9651

potential application being the creation of arrays of deformable, yet well-defined nanopores which could detect a variety of differently sized molecules, as opposed to having a single, static nanopore. Second, the observation of ionic fluid phase transitions in these less well-defined nanopore structures shows the possibility of experimentally observing phase transitions in other interesting natural and synthetic porous systems, such as rocks and concrete. Finally, we have evaluated several potential mechanisms of stochastic pore-blocking in nanopores, including phase transitions, Coulter blocking, and nanoprecipitation—these experiments will be useful for characterizing future nanopore systems.

■ ASSOCIATED CONTENT

Supporting Information

Details of the patch clamp setup, AFM images of flat PDMS surfaces, surface charge density calculations for native PDMS, surfactant charge density calculations, temperature experiment results, effects of vibration, and results of individual patch clamp measurements. This material is available free of charge via the Internet at http://pubs.acs.org.

■ AUTHOR INFORMATION

Corresponding Author

*E-mail strano@mit.edu (M.S.).

Notes

The authors declare no competing financial interest.

■ ACKNOWLEDGMENTS

This work was funded by a grant from British Petroleum (BP) and Siemens. D.B. acknowledges support from the NDSEG Fellowship.

■ REFERENCES

(1) Bezrukov, S. M.; Vodyanoy, I.; Parsegian, V. A. Counting Polymers Moving Through a Single Ion Channel. *Nature* **1994**, *370* (6487), 279–281.

(2) Storm, A. J.; Chen, J. H.; Ling, X. S.; Zandbergen, H. W.; Dekker, C. Fabrication of Solid-State Nanopores with Single-Nanometre Precision. *Nat. Mater.* **2003**, *2* (8), 537–540.

(3) Ito, T.; Sun, L.; Henriquez, R. R.; Crooks, R. M. A Carbon Nanotube-Based Coulter Nanoparticle Counter. *Acc. Chem. Res.* **2004**, *37* (12), 937–45.

(4) Kasianowicz, J. J.; Robertson, J. W. F.; Chan, E. R.; Reiner, J. E.; Stanford, V. M. Nanoscopic Porous Sensors. *Annu. Rev. Anal. Chem.* **2008**, *1* (1), 737–766.

(5) Lee, C. Y.; Choi, W.; Han, J.-H.; Strano, M. S. Coherence Resonance in a Single-Walled Carbon Nanotube Ion Channel. *Science* **2010**, *329* (5997), 1320–1324.

(6) Choi, W.; Lee, C. Y.; Ham, M.-H.; Shimizu, S.; Strano, M. S. Dynamics of Simultaneous, Single Ion Transport through Two Single-Walled Carbon Nanotubes: Observation of a Three-State System. *J. Am. Chem. Soc.* **2010**, *133* (2), 203–205.

(7) Ulissi, Z. W.; Shimizu, S.; Lee, C. Y.; Strano, M. S. Carbon Nanotubes as Molecular Conduits: Advances and Challenges for Transport through Isolated Sub-2 nm Pores. *J. Phys. Chem. Lett.* **2011**, *2* (22), 2892–2896.

(8) Powell, M. R.; Cleary, L.; Davenport, M.; Shea, K. J.; Siwy, Z. S. Electric-Field-Induced Wetting and Dewetting in Single Hydrophobic Nanopores. *Nat. Nanotechnol.* **2011** (Oct), 1–5.

(9) Dekker, C. *Solid-State Nanopores* **2007**, *2* (4), 209–215.

(10) Hou, X.; Zhang, H.; Jiang, L. Building Bio-Inspired Artificial Functional Nanochannels: From Symmetric to Asymmetric Modification. *Angew. Chem., Int. Ed.* **2012**, *51* (22), 5296–5307.

(11) Sakmann, B.; Neher, E. Patch Clamp Techniques for Studying Ionic Channels in Excitable Membranes. *Annu. Rev. Physiol.* **1984**, *46* (1), 455–472.

(12) Sachs, F.; Qin, F. Gated, Ion-Selective Channels Observed with Patch Pipettes in the Absence of Membranes: Novel Properties of a Gigaseal. *Biophys. J.* **1993**, *65* (3), 1101–7.

(13) Grzywna, Z. J. S.; Liebovitch, L.; Siwy, Z. A Dual Mode Mechanism of Conductance through Fine Porous Membranes. *J. Membr. Sci.* **1998**, *145* (2), 253–263.

(14) Chen, C.-C.; Zhou, Y.; Baker, L. A. Scanning Ion Conductance Microscopy. *Annu. Rev. Anal. Chem.* **2011**.

(15) Behrends, J. C.; Fertig, N. Planar Patch Clamping. In *Patch Clamp Analysis*, 2nd ed.; Walz, W., Ed.; Humana Press: 2007.

(16) Lev, A. A.; Korchev, Y. E.; Rostovtseva, T. K.; Bashford, C. L.; Edmonds, D. T.; Pasternak, C. A. Rapid Switching of Ion Current in Narrow Pores: Implications for Biological Ion Channels. *Proc. R. Soc. London, Ser. B: Biol. Sci.* **1993**, *252* (1335), 187–192.

(17) Pasternak, C. A.; Bashford, C. L.; Korchev, Y. E.; Rostovtseva, T. K.; Lev, A. A. Modulation of Surface Flow by Divalent Cations and Protons. *Colloids Surf., A* **1993**, *77* (2), 119–124.

(18) Lisensky, G. C.; Campbell, D. J.; Beckman, K. J.; Calderon, C. E.; Doolan, P. W.; Rebecca, M. O.; Ellis, A. B. Replication and Compression of Surface Structures with Polydimethylsiloxane Elastomer. *J. Chem. Educ.* **1999**, *76* (4), 537.

(19) Merkel, T. C.; Bondar, V. I.; Nagai, K.; Freeman, B. D.; Pinnau, I. Gas Sorption, Diffusion, and Permeation in Poly(dimethylsiloxane). *J. Polym. Sci., Part B: Polym. Phys.* **2000**, *38* (3), 415–434.

(20) Randall, G. C.; Doyle, P. S. Permeation-Driven Flow in Poly(dimethylsiloxane) Microfluidic Devices. *Proc. Natl. Acad. Sci. U. S. A.* **2005**, *102* (31), 10813–10818.

(21) Peter, C.; Hummer, G. Ion Transport through Membrane-Spanning Nanopores Studied by Molecular Dynamics Simulations and Continuum Electrostatics Calculations. *Biophys. J.* **2005**, *89* (4), 2222–2234.

(22) Ho, C.; Qiao, R.; Heng, J. B.; Chatterjee, A.; Timp, R. J.; Aluru, N. R.; Timp, G. Electrolytic Transport through a Synthetic Nanometer-Diameter Pore. *Proc. Natl. Acad. Sci. U. S. A.* **2005**, *102* (30), 10445–10450.

(23) Smeets, R. M. M.; Keyser, U. F.; Krapf, D.; Wu, M.-Y.; Dekker, N. H.; Dekker, C. Salt Dependence of Ion Transport and DNA Translocation through Solid-State Nanopores. *Nano Lett.* **2006**, *6* (1), 89–95.

(24) Buyukdagli, S.; Manghi, M.; Palmeri, J. Ionic Capillary Evaporation in Weakly Charged Nanopores. *Phys. Rev. Lett.* **2010**, *105* (15), 158103.

(25) Powell, M. R.; Sullivan, M.; Vlassiouk, I.; Constantin, D.; Sudre, O.; Martens, C. C.; Eisenberg, R. S.; Siwy, Z. S. Nanoprecipitation-Assisted Ion Current Oscillations. *Nat. Nanotechnol.* **2008**, *3* (1), 51–57.

(26) Beckstein, O.; Sansom, M. S. P. Liquid-Vapor Oscillations of Water in Hydrophobic Nanopores. *Proc. Natl. Acad. Sci. U. S. A.* **2003**, *100* (12), 7063–8.

(27) Allen, R.; Melchionna, S.; Hansen, J.-P. Intermittent Permeation of Cylindrical Nanopores by Water. *Phys. Rev. Lett.* **2002**, *89* (17), 2–5.